

Onset of nonlinearity and yield strain of a model soft solid

**Vijesh Tanna, Casey Wetzel &
H. Henning Winter**

Rheologica Acta

ISSN 0035-4511

Volume 56

Number 6

Rheol Acta (2017) 56:527-537

DOI 10.1007/s00397-017-1013-4



Your article is protected by copyright and all rights are held exclusively by Springer-Verlag Berlin Heidelberg. This e-offprint is for personal use only and shall not be self-archived in electronic repositories. If you wish to self-archive your article, please use the accepted manuscript version for posting on your own website. You may further deposit the accepted manuscript version in any repository, provided it is only made publicly available 12 months after official publication or later and provided acknowledgement is given to the original source of publication and a link is inserted to the published article on Springer's website. The link must be accompanied by the following text: "The final publication is available at link.springer.com".



Onset of nonlinearity and yield strain of a model soft solid

Vijesh Tanna¹ · Casey Wetzel² · H. Henning Winter^{1,2}Received: 22 November 2016 / Revised: 23 March 2017 / Accepted: 1 April 2017 / Published online: 20 April 2017
© Springer-Verlag Berlin Heidelberg 2017

Abstract For soft solids with their low modulus, small stress already results in large strain, which may cause nonlinearity and yielding. These potentially competing effects were studied on a clay/polybutadiene (clay/sPB) composite, which is a soft physical gel. Structural changes were introduced by oscillatory shear using large amplitude (LAOS). LAOS beyond a critical limit reduced the internal connectivity. This softened the already soft solid even further, thereby moving it closer to its physical gel point. For clay/sPB, the shear-induced changes were irreversible so that they could get probed using small amplitude shear (SAOS) frequency sweeps. Sequences of SAOS-LAOS-SAOS (SLS) were repeated with increasing LAOS amplitude and increasing duration. The flow-induced structural changes in the soft solid were attributed to yielding, which began to occur at about the same stress/strain values as found for the onset of nonlinearity in traditional SAOS to LAOS (StL) stress amplitude sweeps. The onset of nonlinearity and the yielding seem to be a strain activated process since the characteristic strain amplitude is independent of frequency and temperature, but not so for the characteristic stress amplitude. The duration of LAOS in a SLS experiment beyond

yielding is an important parameter since flow-induced structural changes require time to grow.

Keywords Yield stress · Linear viscoelasticity · Oscillatory shear · Nonlinearity · Reverse gelation

Introduction

The concept of yielding has been introduced by Bingham (1916). A special issue of *Rheologica Acta* celebrate the centennial anniversary of Bingham's seminal paper (Coussot et al. 2017). Soft solid material such as foams, gels, colloids, and soft composites, because of their low modulus, can yield already when exposed to small stress. Nonlinearity of viscoelastic properties sets in upon small stress/strain. Both phenomena need to be considered and related to each other for a deeper rheological understanding. Lightly cross-linked chemical gels have been shown to rupture internally and undergo a solid to liquid transition when subjected to shear stress as low as 100 Pa (Venkataraman and Winter 1990). Yield stress of similar magnitude has been reported (200 Pa) in a block copolymer/clay composite (Krishnamoorti et al. 2001). Shear-induced yielding may irreversibly change the internal connectivity and/or possibly generate alignment of the sample's constituents. Further examples are the shear-induced alignment of block copolymers (Scott et al. 1992, Koppi et al. 1992) or the homogenization of composites.

A material's relaxation modulus, $G(t)$, describes all of linear viscoelasticity (Boltzmann 1876). The linear viscoelastic (LV) properties are unaffected by the imposed stress or strain as long as the applied stress and strain is small enough. However, a key question, which arises, is how small the applied stress or strain should be? One may also ask how this stress or strain limit can best be measured and by how much its

Part of the special issue: Yield Stress Fluids: a 100 Years after Bingham's Landmark Paper

Electronic supplementary material The online version of this article (doi:10.1007/s00397-017-1013-4) contains supplementary material, which is available to authorized users.

✉ H. Henning Winter
winter@umass.edu

¹ Department of Polymer Science and Engineering, University of Massachusetts Amherst, Amherst, MA 01003, USA

² Department of Chemical Engineering, University of Massachusetts Amherst, Amherst, MA 01003, USA

value changes over a given time span or frequency. Defining the most sensitive way to decouple linear and nonlinear terms remains a significant challenge because nonlinear terms can never be thought of as being perfectly zero but instead as being negligible at low enough strains.

For most viscoelastic materials, the strain limit of LV is very small, $\gamma \ll 1$, and as a consequence higher order terms, which depend on $\gamma^2 \ll \gamma$, $\gamma^3 \ll \gamma$, remain insignificant for LV experiments. Viscoelastic material functions which depend on γ dominate over material functions which depend on γ^2 or γ^3 . Examples of such higher order terms are the first normal stress coefficient in shear (Laun 1978)

$$N_1 \sim \gamma^2 \quad (1)$$

and the third harmonic response to small amplitude oscillatory shear (Hyun et al. 2002, Cziep et al. 2016).

$$I_3 \sim \gamma^3 \quad (2)$$

With increasing stress or strain, the square and cube dependent material functions begin to contribute in a more significant manner. Precise measurements and an ideal material system might be able to quantifiably describe and define when the onset of nonlinear terms begins to contribute in a significant enough manner.

This experimental study tries to effectively identify the onset of nonlinearity for a soft model material. Different LV material functions show different sensitivity to large stress or strain. Oscillatory shear experiments at small amplitude (SAOS) and at large amplitude (LAOS) were chosen for this study since they have been used extensively to characterize viscoelastic properties of liquids and solids, and to detect the onset of nonlinearity. SAOS and LAOS experiments can be performed independently of the type of material and will be applied here to a model soft solid, which undergoes reverse gelation under shear.

In one set of oscillatory shear experiments, we begin at small strain or stress and steadily increase the amplitude. Such a SAOS to LAOS strain/stress ramp (StL) starts well below its critical amplitude where a LV baseline is established. The larger and larger stress/strain amplitudes then drive the sample into its nonlinear regime. Typically, deviations from the LV baseline identify the critical stress/strain at which a sample enters its nonlinear regime. Parameters are sampling density and frequency. In another set of oscillatory shear experiments, we alter the sample's structure by stepwise increasing the LAOS stress amplitude and the LAOS exposure time, and then use SAOS to monitor the LAOS-induced structural changes. The SAOS-LAOS-SAOS (SLS) experiment will be applied in the second part of the paper.

For StL experiments, yielding has been defined by the crossover of the storage and loss modulus (Shih et al. 1999), a maximum in stress amplitude (Yang et al. 1986), or the

downturn of the modulus beyond a critical stress or strain amplitude (Mason et al. 1996). In all such instances, the rheological response is associated with structural changes. However, it is fair to question whether any nonlinear deformation has occurred prior to yielding (i.e., onset of nonlinearity = yield stress/strain?). The naturally occurring recovery dynamics of most materials make it difficult to argue any of these criteria. In many instances, one of the above-mentioned analytical methods is selected to define yielding and used throughout a given study.

Little attention has been devoted to the effect of frequency on yield stress or strain. A change in frequency raises or lowers the LV baseline and, thus, may also affect the yielding behavior. For a fumed silica electrolyte gel, the yield stress has been shown to be unaffected by frequency (Walls et al. 2003). However, for hard sphere colloidal glasses and thermosensitive soft core-shell colloid, the yield strain increased with frequency (Petekidis and Vlassopoulos 2003, Carrier and Petekidis 2009). Both yield stress and strain showed a power law dependence with frequency in soft colloidal glasses of star polymer solutions (Helgeson et al. 2007). The diverse nature of yielding both in terms of types of materials tested and their relationship with key experimental parameters, presents a need for a detailed study in model materials.

The novelty in this research lies in the use of a soft solid material, which irreversibly changes upon exposure to large stress or strain. Such a property was found in a clay/polymer composite, in which the clay had been exfoliated in a polybutadiene matrix. Exfoliation causes the material to form a physical gel (Momani et al. 2016), which however loses some of its internal connectivity under shear (reverse gelation). The material is able to have a quantifiable stress history imprinted upon it. It “memorizes” if it was ever exposed to large strain. Structural changes are irreversible and can be quantified with SAOS by using the baseline of measured rheological material functions as reference. A major challenge was to load the unexfoliated sample into the rheometer fast enough before it develops its shear-sensitive structure. StL experiments provided values for the onset of nonlinearity and SLS generated progressive states of yielding. Once the dependence on LAOS exposure time and LAOS amplitude was established, we used StL and SLS to quantify the LAOS frequency dependence of yielding/nonlinearity. Results from this work suggest that yielding of the clay/polymer composite is a strain activated process.

Experimental

Materials

The soft solid sample in this study consists of an exfoliated organoclay in a matrix of “sticky” end-functionalized

polybutadiene (sPB), which is a dicarboxy terminated polybutadiene with $M_n = 4200$ g/mol (Sigma-Aldrich). Organically modified montmorillonite clay (DK1), purchased from Fenghong Clay Corporation, had its sodium counterion substituted with octadecyltrimethyl ammonium. Samples for this study were prepared with a DK1/sPB ratio of 10/90 wt%. An additional 0.2 wt% of Irganox B225 (BASF) served as antioxidant to minimize degradation of the polymer. Further material description can be found in the literature (Zhu et al. 2007).

Sample preparation

Sample preparation and rheometer loading followed a time-controlled sequence of steps. The sample preparation started with massing the components and gently homogenizing the mixture in a Flacktek planetary mixer at 3000 RPM for 45 s. This ensured a consistent mixing quality (reproducible rheological properties) without breaking the clay aggregates into individual particles. Immediately after mixing, samples were loaded into the rheometer, which was then set to the prescribed gap height of the cone-plate geometry. Up to this state, the sample is still a liquid. For a short while, a freshly mixed sample is nothing more than a suspension. Short timing between steps is required so that the sample loading and gap setting are completed before significant intercalation/exfoliation could occur. We took advantage of the fact that exfoliation requires time. The mixing and rheometer loading occurred at ambient temperature where exfoliation is slow (Momani et al. 2016). After having loaded the sample, annealing at 80 °C for 8 h allowed the clay to fully exfoliate, at which point the composite had reached a physically cross-linked solid state (physical gel). Similar sample preparation sequences have been used by others along with full morphological characterization of the exfoliated composite (Zhu et al. 2007, Chen et al. 2005, Zhu et al. 2007).

The above prescribed method presents a standardized way to generate samples which are unaffected by the mixing and/or by the sample loading into the rheometer. A reproducible starting condition was achieved for our oscillatory shear experiments. However, a new “virgin” sample, free of stress history, had to be prepared for each of rheological experiments of this study.

Oscillatory shear measurements

A stress-controlled rotational rheometer (Malvern Kinexus Pro+), with a cone and plate geometry of 40-mm-plate diameter and 4° cone angle, was used to achieve uniform shear. All SAOS measurements were carried out in strain controlled mode at low strain values of 0.1%. Specific experimental conditions and parameters will be discussed in the result section.

Results

Shear sensitivity of soft solid structure

SAOS master curves on the exfoliated “virgin” sample identify it as a soft solid (physical gel) with a low frequency plateau of the storage modulus, G' , (Fig. 1, circles). In comparison, the lower modulus curves in Fig. 1 (squares) highlight the effect of shear on the clay/sPB structure. The same sample had been sheared at large amplitude (LAOS) for a defined period of time ($\gamma = 1.5$, $\omega = 1$ rad/s, $T = 25$ °C) and afterwards characterized with a SAOS. The drop in modulus and the frequency shift are significant.

Also important is the irrecoverable nature of the composite's structural change. While keeping the shear-modified sample in the rheometer, the sample was allowed to rest for 5 h and SAOS was repeated. The corresponding storage and loss moduli curves (Fig. 1, crosses) are practically identical to the measurement immediately after shearing (Fig. 1, squares). No noticeable recovery occurred in the LV properties during 5 h rest. The sample is still a soft solid, but some of the connectivity in the gel had been reduced permanently. In this way, shear effects are imprinted in the sample and can be rheologically quantified. This property is advantageous for the study of yielding as described further below.

Critical stress/strain determined by SAOS to LAOS transition

Oscillatory shear stress ramps (StL) were performed on “virgin” clay/sPB composites with the objective of finding the stress/strain limit beyond which the sample was driven out of its LV regime. Each StL experiment needed a new sample. Stress amplitudes were increased in steps of constant size on a logarithmic scale, from 0.01 to 10,000 Pa, with a 20 s equilibration time between data points. At each discrete StL stress, the sample was sheared for 40 s. The LV material functions in Fig. 2 express the shear-induced change. Within the LV regime, the dynamic moduli gradually decay with stress amplitude, but then drop off quickly beyond a critical stress amplitude due to a sample's nonlinear response. The linear scale in Fig. 2 amplifies the noise and sample variations.

The StL sampling density varied between 3 (Fig. 2, circles), 10 (Fig. 2, squares), and 20 (Fig. 2, crosses) points per stress decade. The time per data point is kept constant which means that experiments with high sampling density take a longer time and, thus, provide the additional time, which is needed for more extensive structural changes. The slight modulus change at low amplitude was always present but could be considered negligible.

The soft solid composite of this study exhibits classical shear thinning behavior, typical for polymer melts and solutions. It is a “type 1” material according to the classification of

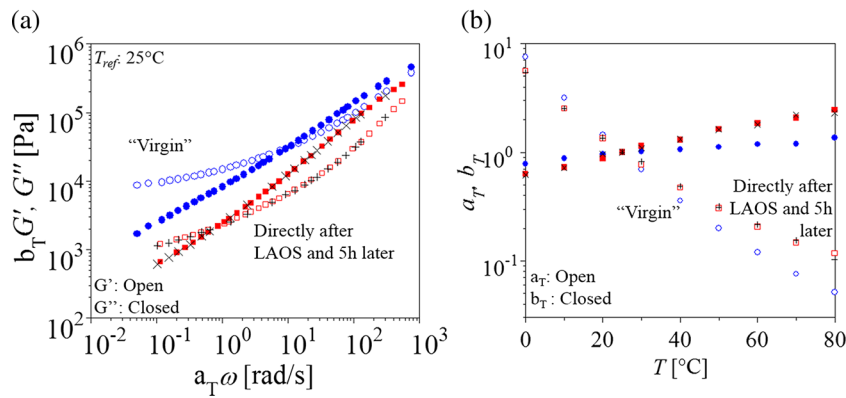


Fig. 1 **a** SAOS master curves of three states of the 90/10 wt% clay/SPB composite—before shear (*circles*), after LAOS shear (*squares*), and after having given the sample 5 h to recover from LAOS (*crosses*). For LAOS shear modification, the sample was subjected to $\gamma = 1.5$, $\omega = 1$ rad/s, $T = 25$ °C. Due to the shearing, the moduli of the virgin sample get

reduced by a factor 0.066, and the relaxation times increase by a factor of about 15. Shearing softens the material considerably and cause relaxation processes to require much more time. **b** Dynamic moduli in the temperature range of 0–80 °C at 10 K intervals were shifted to $T = 25$ °C. The vertical temperature shift factor is close to 1

Hyun et al. (2002). Both the storage and loss moduli drop, but the storage modulus begins to decay at a lower stress than the loss modulus and does so at a faster rate, a phenomenon reported for several materials (Salehiyan and Hyun 2013, Derkach et al. 2015). Surprisingly, the onset of nonlinearity seems to depend on sampling density. This will need to be explained. We attribute this phenomenon to the time dependence of structure rearrangements. The StL stress amplitude increases much faster at low sampling density and thus allows less time for the growth of new structural states. Consequently, a low sampling density (faster sweep) gives the appearance of an extended LV region.

The deviations from linearity are gradual. This makes it difficult to assign a meaningful stress or strain limiting value for the onset of nonlinearity. To explore this question in detail, we apply a continuous and a discrete method to determine how best to describe the onset. In addition, two LV material functions were studied which address a key question, as to whether an additive function, $G^* (= \sqrt{G'^2 + G''^2})$, or a multiplicative function, $\tan\delta$, is more appropriate and sensitive to

predicting nonlinearity. For the following analysis, we selected both, G^* and $\tan\delta$. Regardless of whether the storage or loss modulus deviates first, the deviation was captured by both functions since each of them depends on both, the storage and the loss modulus, but in different ways.

In our first approach, we express G^* and $1/\tan\delta$ with a nonlinear continuous empirical fitting function and the gradient of that function

$$y = \frac{y_b}{(1 + (Bx)^a)^{b/a}}; \frac{\partial \log y}{\partial \log x} = \frac{-b(Bx)^a}{(1 + (Bx)^a)} \quad (3)$$

in which y represents G^* and $1/\tan\delta$, respectively, and x was set equal to σ_a or γ_a . The form of this function was inspired by Carreau-Yasuda model (Yasuda et al. 1981). To preserve the general shape for all material functions (downturn due to yielding), we opted to fit $1/\tan\delta$ rather than $\tan\delta$. The LV baseline values are captured in the y_b parameter. Fitting parameters, a , b , B , and y_b were optimized with the IRIS software (Winter and Mours 2006). As onset criterion, a 5% deviation from the LV baseline was chosen, $y = 0.95 y_b$. The log-

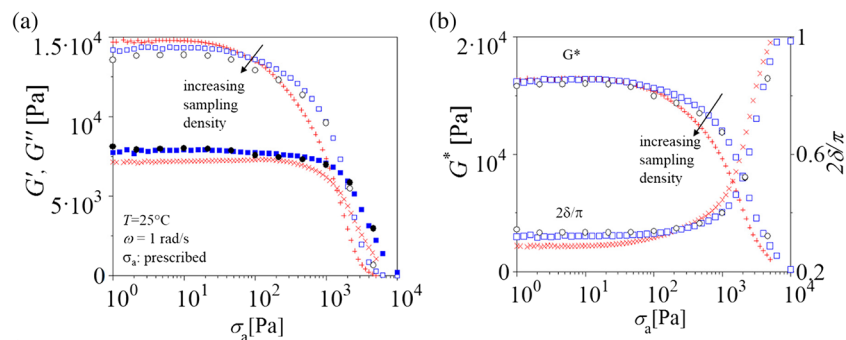


Fig. 2 SAOS stress sweeps (StL) at varying sampling densities plotted with a variety of material functions using linear scaling. **a** Shows the storage and loss moduli and **b** the complex and tangent function. Each LV function provides a nice LV baseline in the low stress regime,

followed by classic shear thinning behavior, which is observed as the sample leaves its LV regime. The onset of nonlinearity occurs at smaller stress/strain when probing with high sampling density (slow sweep). Isothermal experiments at 25 °C at 1 rad/s

log gradient of the fit function, $\delta \log y / \delta \log x$, served as a second criterion. A value of 0.05 in the log-log scale was chosen to identify the onset stress and strain. Figures 3a, b show the calculated stress and strain values from these criteria. As the sampling density increased, the onset stress and strain decreased for both G^* and $\tan\delta$ with this criterion. The variation in onset values is much more extreme in the case of $\tan\delta$ than in G^* . Generally, the values from both gradients give lower critical onset values. The onset stress values ranged from 99.6–542 Pa and strains from 0.42–3.2%.

Instead of using an analytical fit function, Eq. 3, the data from Fig. 2 can also be analyzed in their original digital format. Such discrete analysis is easier to perform. For a given material function, a baseline was established by averaging discrete data points in the linear portion of the SAOS stress sweeps. The onset of nonlinearity was found, by our definition here, when the sample deviated from its baseline by 5%. The two data points before and after the deviations, (γ_1, σ_1) and (γ_2, σ_2) , defined the region of nonlinear onset, meaning that the onset of nonlinearity occurred at some value in between these two points. A meaningful value for the onset stress was found by linear interpolation between σ_1 and σ_2 . The interpolated value at which a 5% deviation occurred was chosen as onset stress, σ_c . The same procedure was repeated for the onset strain.

A discretized log-log gradient was defined as

$$\frac{\partial \log(y)}{\partial \log(x)} = \frac{\log y_{n+1} - \log y_n}{\log x_{n+1} - \log x_n} \quad (4)$$

Wherever the gradient value exceeded 0.05, two neighboring data points were identified and the abovementioned linear interpolation was repeated to find the onset stress/strain. The resulting values from this method are shown in Fig. 4. All onset stresses/strains from the discrete method fluctuate only slightly with respect to sampling density. All onset stresses from this method were found to be between 77 and 177 Pa and with strains from 0.43–1.24%. These values are quite low when compared to values from equation fitting. While it is not

as clear as in the case of continuous fitting method, G^* again appears to express lower onset values than $\tan\delta$. This leads us to the conclusion that perhaps G^* , an additive type function, is more appropriate when defining the onset of nonlinearity than $\tan\delta$, a multiplicative function. Furthermore, the gradient method once again assigns lower onset values for the crucial stress and strain.

When comparing the onset stress/strain values from this analysis, it appears that both the fitting function and the discrete method predict similar values for high sampling density. However, the fitting function predicts higher onset stresses/strains at low sampling densities meaning great care must be taken when defining experimental parameters. For the remainder of this study the gradient of the discrete baseline method will be used to identify the onset of nonlinearity. This method suggests low onset values, which appear to be independent of sampling density. Ten samples per decade will be used for the remainder of the study.

Yielding determined by SAOS-LAOS-SAOS

A key feature of the clay/SPB composite is that once yielded under sufficient stress or strain, it is unable to recover its virgin structure. It undergoes an irreversible structural transition, of which we take advantage in the following way. Each experiment starts with a virgin sample. We periodically expose the sample to brief periods of LAOS. Before and after each LAOS application, the sample is characterized with SAOS frequency sweep for LV characterization. In this way, we systematically characterize the effect of the imposed deformation. A similar characterization has been used in previous studies in which structural characterization were performed using microscopy rather than SAOS (Hu et al. 1998, Franceschini et al. 2014). Strain amplitude and duration of the applied deformation are the two user defined parameters in such an SLS experiment (see Fig. 5). Such a method is not limited to LAOS deformations and other potential deformation mechanism will be addressed in the future. In our first experiments, SLS were

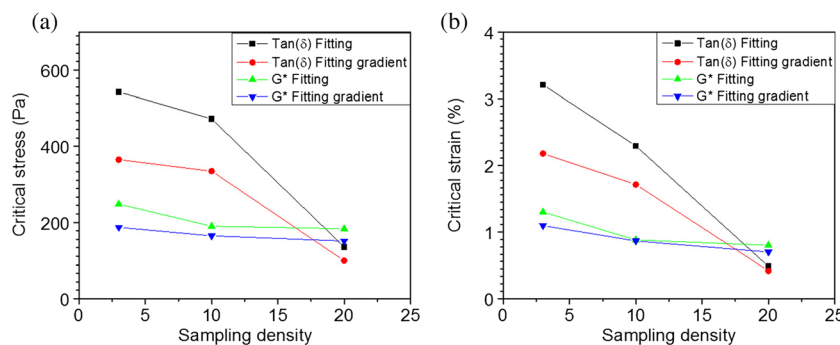
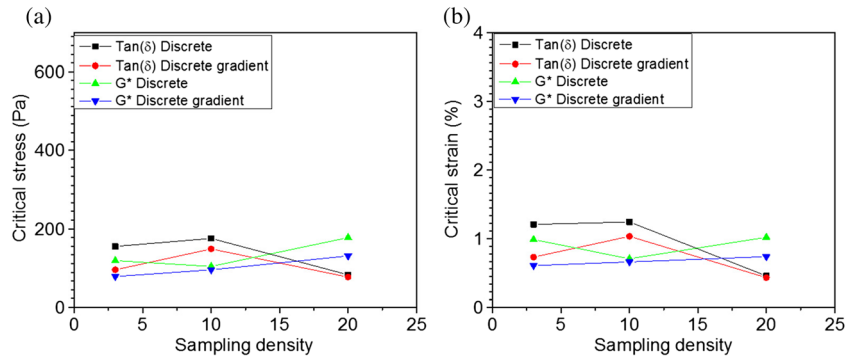


Fig. 3 The onset stress (a) and onset strain (b) amplitudes calculated from $y(x)$ and the gradients (Eq. 3) based on data from Fig. 2. Both G^* and $\tan\delta$ fit functions and their gradient were used. As the sampling

density increased, the onset stress/strain decreased, which indicates the importance of exposure time at increased stress/strain as will be discussed below

Fig. 4 The onset stress (a) and onset strain (b) amplitudes when applying the discrete baseline method and gradient value criteria. Both G^* and $\tan\delta$ were used to study the discrete baseline method using the direct method and gradient (Eq. 4)



repeated multiple times while changing strain amplitude and maintaining constant deformation times. In the second experiment, we varied the LAOS duration while maintaining a constant strain amplitude. Both, increasing strain amplitude and increasing LAOS time lead to irreversible structural changes once a critical stress or strain amplitude is exceeded and the sample yields, i.e., causes the sample to flow.

Thirteen SLS cycles with incrementally increasing strain amplitudes (during the LAOS step) were performed at room temperature. Each deformation cycle lasted 30 min and was carried out at 1 rad/s. Initially, the applied strain was kept below sample's onset strain ($\gamma_A < \gamma_d$) as learned from the StL transition behavior. The increasing strain amplitudes eventually exceed the critical strain ($\gamma_A > \gamma_d$). Frequency sweeps were applied after each LAOS period. At low strain amplitudes, only small deviations are seen (highlighted further in the figure inserts) while larger strain amplitudes become effective in lowering the moduli and thereby indicating a loss in connectivity as demonstrated in Booij-Palmen (Fig. 6a) and Winter plots (Fig. 6b) (Booij and Palmen 1982, Winter 2009). Both plots effectively highlight deviations from the virgin sample. The Booij-Palmen plot (Booij and Palmen 1982) indicates that a traditional horizontal shift does not superimpose the shear modified clay/sPB. An additional vertical shift is needed as will be shown below. The Winter plot (Winter 2009) is known to magnify any transition in the material, thus highlighting the connectivity reduction in clay/sPB while maintaining its solid properties when probed in SAOS.

To further highlight the deviations from the virgin sample, the SAOS moduli after each LAOS application were subtracted from the initial moduli of the virgin sample. The storage (Fig. 7a) and loss modulus (Fig. 7b), after the subtraction, begin to deviate mostly at high frequencies. Deviations eventually extend out to the low frequency regime as the strain amplitude was further increased. The first strain at which a deviation is observed at all frequencies is 0.75%. For the purpose of this study, we will say the deviation occurred somewhere between 0.5–0.75%. This value agrees well with the values calculated from the gradient of discrete baseline in the previous section, indicating that the onset of nonlinearity corresponds to beginning of yield.

Time dependence of structural change during yielding

Yielding involves flow and flow needs time. The duration of exposure to LAOS turned out to be an important parameter. The gradual change due to LAOS was monitored by exposing a fresh sample to 45 SLS cycles at a constant LAOS strain amplitude of $\gamma_a = 0.1$ for 2 min at 1 rad/s. This LAOS step consisted of approximately 35 oscillatory rotations. A strain amplitude was chosen well above the sample's yield strain to ensure rapid structure evolution. Since the sample is unable to recover we can treat each LAOS time from each cycle as additive. As the duration of LAOS increased, LV properties changed significantly (see Fig. 8). The dynamic moduli decreased and characteristic relaxation times increased due to

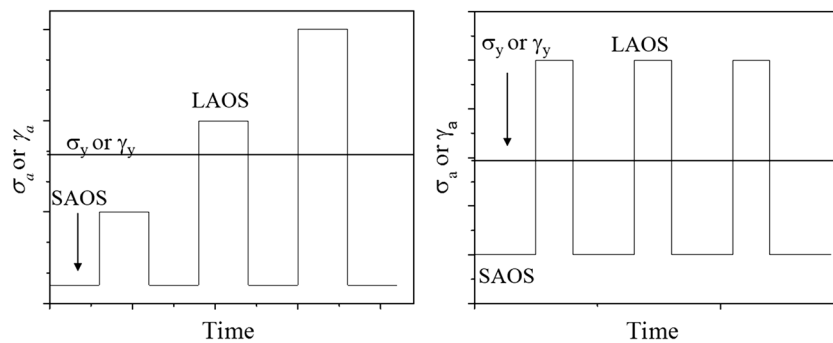
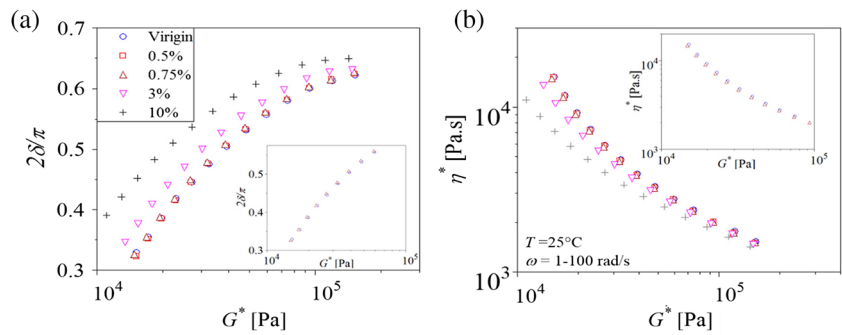


Fig. 5 Timing of the SAOS-LAOS-SAOS (SLS) method in which large stress/strain amplitudes are used to alter the sample's structure and SAOS to rheologically probe the evolving structure. The LAOS amplitude is

increased in a stepwise fashion (left) or the LAOS exposure time is increased in additive fashion (right)

Fig. 6 SAOS frequency sweeps after LAOS applications at stepwise increasing amplitude, expressed in a Booiij-Palmen (a) and Winter plot (b). LAOS was applied for 30 min each at $\omega = 1$ rad/s. Only selected SAOS data are shown



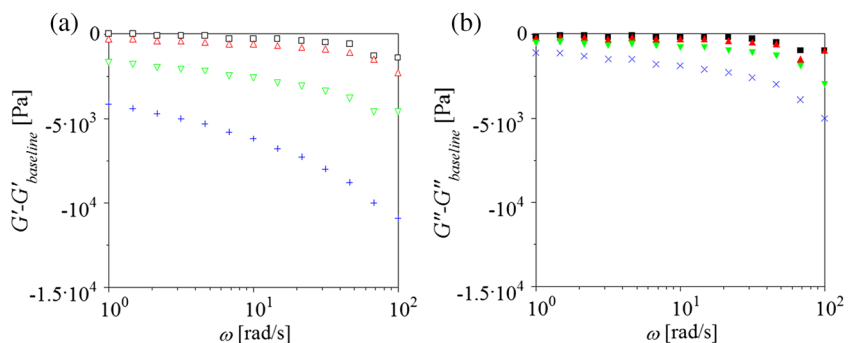
yielding. Eventually at long deformation times, it appears that the sample's LV properties approach saturation.

The LAOS shearing time per cycle was kept constant (2 mins). The overall LAOS time increased with each shearing period. SAOS provided G' , G'' data, which we then shifted by LAOS-time-time superposition with the virgin sample as reference. In that narrow frequency range, the dynamic moduli superimpose quite well in a self-consistent manner (Fig. 9a). Both horizontal, a_2 , and vertical, b_2 , shifting is required. If horizontal shifting by itself would be sufficient, the Booiij-Palmen plot would already merge all curves into a single mater curve. This is not the case. A substantial vertical shift is also required. The corresponding shift factors are plotted in Fig. 9b. Initially, a large shift is observed indicating a fast drop in modulus and a substantial increase of the relaxation times. Even after 90 min of exposure to the LAOS, the shift factors are still changing slightly, meaning a fully developed state at that shearing intensity has not been reached. This further indicates the importance of time evolution associated with yielding.

Effect of frequency on nonlinearity and yielding

Up to here, all StL amplitude sweeps were shown for a single frequency (1 rad/s). However, frequency is an important parameter. StL measurements at 4 different frequencies of 0.42, 1, 4.2, and 10 rad/s showed that varying frequency strongly affects a sample's storage and loss modulus. Both increase with frequency (Fig. 10). Superficially, the trends look pretty much the same for both strain (Fig. 10a) and stress (Fig. 10b).

Fig. 7 Storage (a) and loss (b) moduli subtracted from the virgin sample's baseline. Data taken from Fig. 6



The sensitivity to large stress or strain becomes more obvious when normalizing the complex moduli with respect to their respective LV baseline (Fig. 11 a, b). This removes the vertical modulus shift due to frequency, which is not the focus of this experiment. In this way, the onset of nonlinearity can be compared for the different frequencies. Fig. 11a shows the data set as a function of strain and Fig. 11b as a function of stress. For our samples, Fig. 11b demonstrates that normalized complex modulus deviate from the LV baseline much “earlier” at low frequencies than at higher frequencies. The samples seem to have a lower yield stress when measuring at low frequencies. This completely changes when plotting the same data against strain (Fig. 11a): the onset of nonlinearity becomes independent of frequency. All curves collapse into a single curve with a single onset value for the strain! This suggests that, for the clay/sPB system, yielding should be thought of as a strain activated process instead of stress activated.

The resulting yield stresses were plotted as a function of frequency. Since yield strains were independent of frequency, they are not shown. A simple power law dependence was used to establish a relationship between yield stress and frequency in Fig. 12.

$$\sigma_y = A \left(\frac{\omega}{\omega_0} \right)^b \tag{5}$$

A , b are fitting parameters and ω_0 is an arbitrary reference frequency. It remains unclear how the fitting parameters are related to the sample's intrinsic properties. A similar

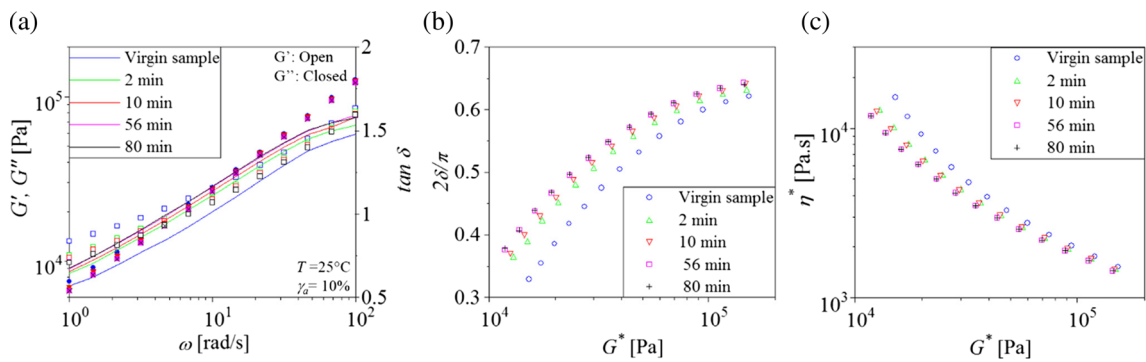


Fig. 8 SAOS frequency sweeps after various LAOS times in modulus and $\tan \delta$ (a), Booy-Palmen (b) and Winter plot (c) The LAOS strain amplitude was $\gamma_a = 0.1$ and the LAOS frequency was 1 rad/s for 2 min

qualitative trend between yield stress/strain was observed when varying the temperature (see supplement). The yield strain was independent of temperature and the yield stress increased when lowering the temperature.

Discussion

The clay/sPB composite turns out to be an ideal material system to study the onset of nonlinearity and yielding in a systematic fashion. Not only is the material a solid with a distinct yield condition but also, once yielded, it is unable to recover its virgin structure. Furthermore, a well-defined initial state is guaranteed for all experiments due to the sample's ability to form its structure after (and not before!) having been loaded into the rheometer. Initially, it is a stress-free solid (physical gel), which then gets deformed uniformly between the cone and plate fixtures, unlike in a parallel plate geometry or the vane tool. Small amplitude oscillatory shear (SAOS) serves as a rheological measure of the evolving structural states as induced by large amplitude oscillatory shear (LAOS). To determine the morphological structural changes associated with yielding the composite would require additional characterization, which is outside the scope of this rheological study.

Two different experimental protocols (StL and SLS) deliver complementary results with respect to the onset of nonlinearity and yielding. The StL experiment applies oscillatory shear at

increasing stress amplitude and causes a transition to nonlinearity. The SLS experimental protocol alternated between SAOS, LAOS, and back to SAOS, and repeated this sequence many times. LAOS treatment and characterization are separated in this way and yielding behavior is decoupled from the onset of nonlinearity. An added benefit of SLS is its ability to probe samples at multiple frequencies (rather than single frequency StL stress ramps). For our sample, both onset of nonlinearity and yielding occurred at about the same strain amplitude between 0.5–0.75%. This suggests that either StL or SLS can be used to detect the onset of yielding.

Repeated StL stress ramps at different frequencies, each with a new sample, indicate that the clay/sPB composite's yielding behavior is a strain activated process, not stress activated (Fig. 10). The onset of nonlinearity, which for our sample appears to be synonymous with yielding, moves to higher stresses for shearing at higher frequencies. A power-law relates yield stress and frequency in the small range of frequencies tested (0.42–10 rad/s). In comparison, the sample's yield strain did not noticeably change with frequency. The same trend (strain activated) held for StL at increased temperature. As the temperature was increased, the yield stress decreased while the yield strain stayed constant. The temperature/frequency stress dependence is self-consistent in that to hit a target strain, a lower stress amplitude is needed for softer samples.

In both, the StL and SLS experiments, LAOS exposure time plays a key role. The experiments are very different but

Fig. 9 Master curve after using LAOS time- time shifting (a) and the corresponding shift factors (b)

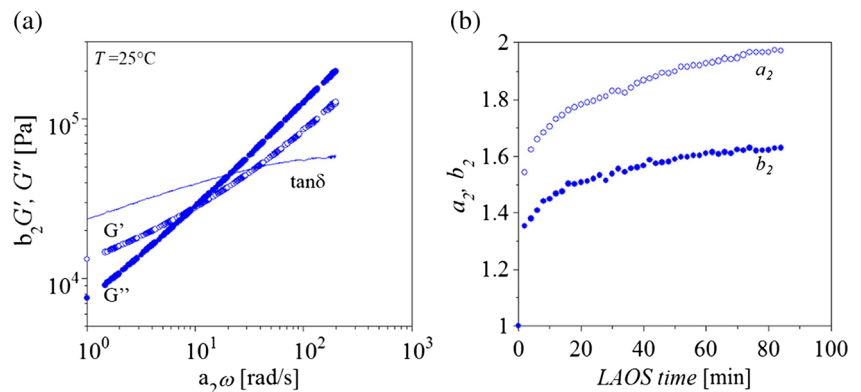
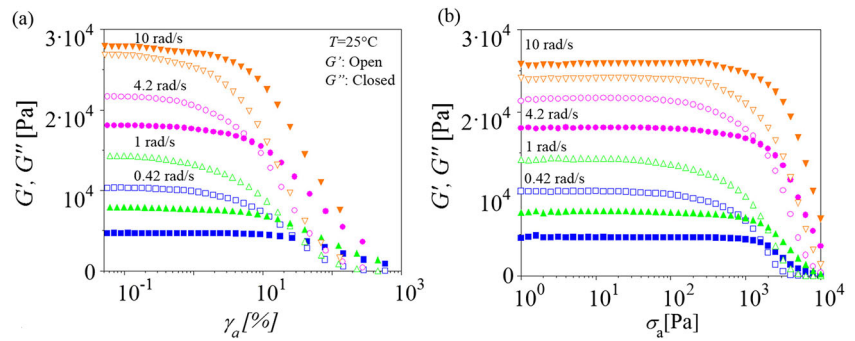


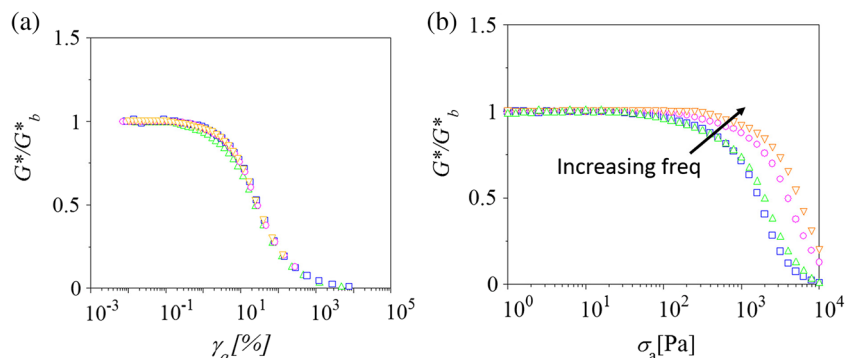
Fig. 10 StL stress sweeps at varying frequencies versus strain (a) and stress (b) amplitudes



the message is consistent. The exposure time increased in StL experiments when increasing the sampling density and in SLS experiments when staying longer in LAOS mode. In StL experiments, a high sampling density resulted in additional time spent at intermediate stresses/strains and, thus, the sample's structure was given more time to adjust. However, even then, StL shearing does not provide sufficient time for the material to reach a fully developed structure. A better option is SLS. For SLS at constant strain amplitude above the yield strain and at larger and larger LAOS exposure times, the material seems to approach a fully developed state (Fig. 9). However, despite applying LAOS for a total of 90 min, the composite structure is still rearranging as expressed in the LV data.

The shear-induced states in the soft clay/polymer composite might best be understood in the context of soft solid rheology near the chemical and/or physical gel point. A solid near its gel point is characterized by a low modulus and long relaxation times. During chemical gelation, when increasing the bond probability beyond the gel point, the characteristic material times decay and the characteristic modulus increases (Vilgis and Winter 1988). This general behavior has been seen in many materials. Examples are an epoxy at varied extent of reaction (Adolf and Martin 1990) or a coacervate at reduced in salt content (Liu et al. 2016). Repeated studies on a wide range of materials suggest universal dynamics of soft solids above their gel point independent of the connectivity mechanism (bond probability in chemical gelation). Our virgin sample is a soft solid well above its gel point. It therefore is not surprising to find these same characteristics during the formation of the clay/SPB composite (Momani et al. 2016).

Fig. 11 Complex moduli of Fig. 8 normalized with respect to their LV baseline value, plotted against strain (a) and stress amplitude (b), respectively. The yield/onset stresses and strains were calculated using the gradient of the discrete baseline method



The general dynamics pattern of gelation also governs the reversal of gelation, as shown schematically in Fig. 13. Even if reverse gelation samples a sequence of structural states which are not the same as in gelation (Venkataraman and Winter 1990), the general rheological pattern is the same for reducing or advancing connectivity. Under yielding condition, the rheology of the clay/SPB composite exhibits the rheological pattern typical for reverse gelation, and this even without actually reaching the gel point from the solid side. Exposure to increased LAOS times causes the clay/SPB to undergo a solid to solid transition. The internal connectivity reduces with LAOS time. Reversed gelation brings the clay/SPB composite closer to its gel point so that the modulus decreases and the relaxation times increase. SAOS frequency sweeps superimpose but require a time shift as well as a modulus shift as already seen with Fig. 1. Both horizontal and vertical shifting is needed to super impose the data.

Previous studies have shown that intercalated organoclay aligns under shear with the consequence of reducing mechanical properties of a clay/polymer composite (Giannelis et al. 1999, Krishnamoorti et al. 2001, Schmidt et al. 2000). We speculate that in our composite, the exfoliated clay sheets orient under the imposed shear and the oriented sheets are separated from each other by the polymer matrix. The reduced particle-particle interaction and reduced direct connectivity between particles leads to the lowering of the modulus as seen in the SAOS data. During reverse gelation, the orientation is expected to develop gradually and should occur at local length scales first, which might be the reason that the orientation effect shows up first in the high frequency tail of the data.

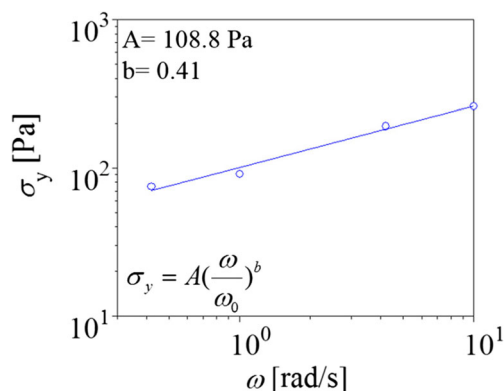


Fig. 12 The yield stress plotted as a function of frequency. A power law was used to relate the two

As the sample is subjected to higher strain and at longer times, more and more clay sheets are expected to orient on a global length scale. As this occurs, shear effects become noticeable at lower frequencies (Fig. 7). The effect of sheet alignment should saturate eventually and LV material functions would become independent of further shearing. As discussed above, long times are required to reach such saturated state. This was not attempted in our experiments, which rather focused on onset conditions.

In future work, we hope to further explore different forms of shear in SLS experiments. Deformations can be performed through LAOS (as done here), steady shear, or a constant stress (if the stress is outside of the LV regime). In this study, LAOS deformation was used. LAOS allowed us to apply large controlled strains for well-defined exposure times. In comparison, creep with periods of large stress would have been a more

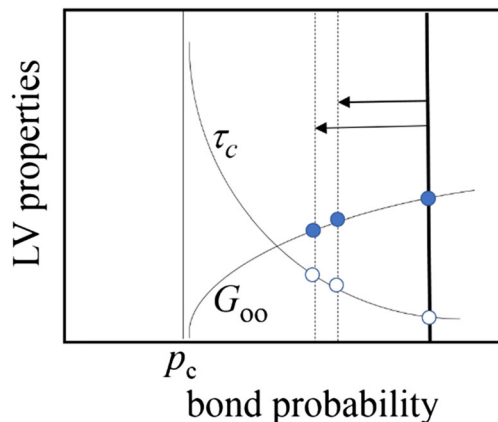


Fig. 13 Schematics of reverse gelation of soft solid above its gel point. Connectivity p_c marks the percolation threshold. In this study, gelation is reversed when shearing the “virgin” sample, which is close to its equilibrium state (marked with a thick vertical line). LAOS shear modification reverses gelation and moves the soft solid closer to its physical gel point. As a consequence, its modulus decreases and its characteristic times get longer after having been exposed to more and more LAOS (larger amplitude, longer times). The magnitude of the shift is shown in Fig. 9b. The term “bond probability” is borrowed from chemical gelation which has been shown to reverse under large strain (Venkataraman and Winter 1990)

conventional way of invoking yield. However, our objective of achieving strains very near the onset of yielding would have required short exposure times and low shear rates. Such short times and shear rates present a challenge (as we learned in preliminary experiments). Both methods do have merits, which we plan to study further.

Conclusions

The clay/sPB composite is a soft solid, which reduces its internal connectivity upon yielding and, hence, is an ideal model system for the study of yielding. Large stress/strain amplitudes result in an irreversible solid to solid transition. When comparing the onset of nonlinearity in a traditional SAOS to LAOS (StL) stress growth experiment with yielding in a SAOS-LAOS-SAOS (SLS) experiment, about the same onset values were found. For our clay/sPB composite, the onset of nonlinearity occurred at about the same strain amplitude as yielding. This yield strain was found to be independent of both frequency and temperature. However, the yield stress increased when increasing the frequency and/or lowering the temperature. An additive function, G^* , was most sensitive to indicate the onset of nonlinearity when comparing to other LV material functions. Yielding allows flow and naturally introduces a time dependence, which became apparent in StL when increasing the stress amplitude more slowly (using higher sampling density) and in SLS when increasing the LAOS time. The finite rate of yielding must be accounted for in experimental planning. When the stress/strain amplitude in StL is raised too quickly, for instance, the LV region appears to be larger than it actually is.

Acknowledgements The research is supported by grant CMMI 1334460 of the National Science Foundation.

References

- Adolf D, Martin J (1990) Time-cure superposition during cross-linking. *Macromolecules* 23:3700–3704
- Bingham ES (1916) An investigation of the laws of plastic flow. *Bull US Bur Stand* 13:309–353
- Boltzmann L (1876) Zur Theorie der elastischen nachwirkung. *Ann Phys Chem* 241:430–432
- Booij HC, Palmen J (1982) Some aspects of linear and nonlinear viscoelastic behavior of polymer melts in shear. *Rheol Acta* 376–387
- Carrier V, Petekidis G (2009) Nonlinear rheology of colloidal glasses of soft thermosensitive microgel particles. *J Rheol* 53:245–273
- Chen T, Zhu J, Li B, Guo S, Yuan Z, Sun P, Ding D, Shi AC (2005) Exfoliation of organo-clay in telechelic liquid polybutadiene rubber. *Macromolecules* 38:4030–4033
- Coussot P, Malkin AY, Ovarlez G (2017) Yield stress — or 100 years of rheology. *Rheol Acta* 56:161–162
- Cziep MA, Abbasi M, Heck M, Arens L, Wilhelm M (2016) Effect of molecular weight, polydispersity, and monomer of linear

- homopolymer melts on the intrinsic mechanical nonlinearity ${}^3Q_0(\omega)$ in MAOS. *Macromolecules* 49:3566–3579
- Derkach SR, Ilyin SO, Maklakova AA, Kulichikhin VG, Malkin AY (2015) The rheology of gelatin hydrogels modified by κ -carrageenan. *LWT-Food Sci Techn* 63:612–619
- Franceschini A, Filippidi E, Guazzelli E, Pine DJ (2014) Dynamics of non-Brownian fiber suspensions under periodic shear. *Soft Matter* 10:6722–6731
- Giannelis EP, Krishnamoorti R, Manias E (1999) Polymer-silicate nanocomposites: model systems for confined polymers and polymer brushes. *Adv Polym Sci* 138:107–147
- Helgeson ME, Norman WJ, Vlassopoulos D (2007) Viscoelasticity and shear melting of colloidal star polymer glasses. *J Rheol* 51:297–316
- Hu YT, Boltenhagen P, Matthys E, Pine DJ (1998) Shear thickening in low-concentration solutions of wormlike micelles. II. Slip, fracture, and stability of the shear-induced phase. *J Rheol* 42:1209–1226
- Hyun K, Kim SH, Ahn KH, Lee SJ (2002) Large amplitude oscillatory shear as a way to classify the complex fluids. *J Non-Newton Fluid Mech* 107:51–65
- Koppi KA, Tirrell M, Bates FS, Almdal K, Colby RH (1992) Lamellae orientation in dynamically sheared diblock copolymer melts. *J Physique II* 2:1941–1959
- Krishnamoorti R, Ren J, Silva AS (2001) Shear response of layered silicate nanocomposites. *J Chem Phys* 114:4968–4973
- Laun HM (1978) Description of the non-linear shear behavior of a low density polyethylene melt by means of an experimentally determined strain dependent memory function. *Rheol Acta* 17:123–129
- Liu Y, Winter HH, Perry SL (2016) Linear viscoelasticity of complex coacervates. *Adv Colloid Interf Sci*. doi:10.1016/j.cis.2016.08.010
- Mason TG, Bibette J, Weitz DA (1996) Yielding and low of monodisperse emulsions. *J Colloid Interface Sci* 179:439–448
- Momani B, Sen M, Endoh M, Wang X, Koga T, Winter HH (2016) Temperature dependent intercalation and self-exfoliation of clay/polymer nanocomposite. *Polymer* 93:204–212
- Petekidis GD, Vlassopoulos PP (2003) Yielding and flow of sheared colloidal glasses. *J Phys Condens Mat* 16:3955–3963
- Salehiyan R, Hyun K (2013) Effect of organoclay on non-linear rheological properties of poly(lactic acid)/poly(caprolactone) blends. *Korean J Chem Eng* 30:1013–1022
- Schmidt G, Nakatani A, Butler P, Karim A, Han C (2000) Shear orientation of viscoelastic polymer-clay solutions probed by flow birefringence and SANS. *Macromolecules* 33:7219–7222
- Scott DB, Waddon AJ, Lin Y, Karasz FE, Winter HH (1992) Shear-induced orientation transitions in triblock copolymer styrene-butadiene-styrene with cylindrical domain morphology. *Macromolecules* 25:4175–4181
- Shih WY, Shih WH, Aksay IA (1999) Elastic and yield behavior of strongly flocculated colloids. *J Am Ceramic Soc* 82:616–624
- Venkataraman SK, Winter HH (1990) Finite shear strain behavior of a crosslinking polydimethylsiloxane near its gel point. *Rheol Acta* 29:423–432
- Vilgis T, Winter HH (1988) Mechanical selfsimilarity of polymers during chemical gelation. *Progr Coll Polym Sci* 26:494–500
- Walls HJ, Caines SB, Sanchez AM, Khan SA (2003) Yield stress and wall slip phenomena in colloidal silica gels. *J Rheol* 47:847–868
- Winter HH (2009) Three views of viscoelasticity for cox-Merz materials. *Rheol Acta* 48:241–243
- Winter HH, Mours M (2006) The cyber infrastructure initiative for rheology. *Rheol Acta* 45:331–338
- Yang M, Scriven LE, Macosko CW (1986) Some rheological measurements on magnetic iron oxide suspensions in silicone oil. *J Rheol* 30:1015–1029
- Yasuda K, Armstrong RC, Cohen RE (1981) Shear-flow properties of concentrated solutions of linear and star branched polystyrenes. *Rheol Acta* 20:163–178
- Zhu J, Wang X, Tao F, Xue G, Chen T, Sun P, Jin Q, Ding D (2007) Room temperature spontaneous exfoliation of organo-clay in liquid polybutadiene: effect of polymer end-groups and the alkyl tail number of organic modifier. *Polymer* 48:7590–7597